

**UNCLASSIFIED**



**Australian Government**

**Department of Defence**

Science and Technology

# Calibration of the DST Group Research Wind Tunnel Pressure Rings

*Jesse McCarthy*

**Aerospace Division  
Defence Science and Technology Group**

DST-Group-TN-1728

## **ABSTRACT**

A calibration of the pressure rings in the DST Group Research Wind Tunnel was performed for an empty test section and with an elevated ground plane installed. This pressure ring system is similar in principle to the piezo-rings utilised in the DST Group Low Speed Wind Tunnel for calculating nominal test-section wind speed with a calibration factor. Calibration factors were obtained for both the empty test section and when the elevated ground plane is installed. It is found that the addition of the elevated ground plane changes the calibration factor significantly.

## **RELEASE LIMITATION**

*Approved for Public Release*

**UNCLASSIFIED**

UNCLASSIFIED

*Produced by*

*Aerospace Division  
506 Lorimer St,  
Fishermans Bend, Victoria 3207, Australia*

*Telephone: 1300 333 362*

*© Commonwealth of Australia 2018  
February, 2018  
AR-017-078*

***APPROVED FOR PUBLIC RELEASE***

UNCLASSIFIED

**UNCLASSIFIED**

# Calibration of the DST Group Research Wind Tunnel Pressure Rings

## Executive Summary

The DST Group Research Wind Tunnel (RWT) has high- and low-pressure rings (i.e. circumferential pressure tappings) installed, similar in principle to the piezo-rings in the DST Group Low Speed Wind Tunnel (LSWT). The high-pressure ring is located before the wind tunnel contraction and the low-pressure ring after the contraction, where the average static pressure is lower than before the contraction. This pressure differential can be measured and calibrated to provide the average wind speed at a downstream station, thus obviating the need for a local wind speed measurement using an intrusive instrument such as a Pitot-static tube.

A calibration of the RWT pressure rings was carried out with a method similar to the LSWT piezo-ring calibration, for the cases of an empty test section and when an elevated ground plane is installed. A first order least-squares fit accounting for errors in both coordinates was used and a calibration constant obtained for each case. The uncertainties in measurements were assessed and found to be within acceptable limits. Thus, the calibration constants may be applied to the pressure ring data and ultimately used for determining wind speed in the RWT test section with or without the elevated ground plane, instead of relying on a pitot-static tube for wind speed measurements.

**UNCLASSIFIED**

**UNCLASSIFIED**

*This page is intentionally blank*

**UNCLASSIFIED**

## Contents

<b>1 INTRODUCTION</b> .....	1
<b>2 RESEARCH WIND TUNNEL DESCRIPTION</b> .....	2
<b>3 TEST EQUIPMENT</b> .....	3
<b>3.1 Pitot-Static Probe</b> .....	3
<b>3.2 Pressure Transducers</b> .....	5
<b>3.3 Temperature Probe</b> .....	5
<b>4 TEST METHODOLOGY</b> .....	6
<b>5 DATA REDUCTION</b> .....	8
<b>6 RESULTS AND DISCUSSION</b> .....	9
<b>7 REFERENCES</b> .....	13
<b>APPENDIX A: SYSTEM UNCERTAINTIES</b> .....	15
<b>APPENDIX B: TABULATED EMPTY TEST SECTION DATA</b> .....	17
<b>APPENDIX C: TABULATED DATA WITH ELEVATED GROUND PLANE     INSTALLED</b> .....	27

## Figures

1 DST Group Research Wind Tunnel.....	2
2 RWT coordinate system.....	3
3 The elevated ground plane supported by the test section walls rather than the four vertical struts. ....	4
4 Photographs of the pitot-static tube fixed to the sting mount inside the RWT for (i) an empty test section, and (ii) with the elevated ground plane installed. ....	4
5 The testing instrumentation and connections used in the calibration. ....	5
6 Least-squares regression fits on empty test section data for (i) baseline and (ii) replicate runs. ....	10
7 Least-squares regression fits on elevated ground plane data for (i) baseline and (ii) rep- licate runs. ....	10

## Tables

1	Pressure ring calibration test matrix.....	7
2	The calibration factors for each RWT test section configuration and the standard error of $q_{ts}$ estimation.....	9
3	Test uncertainties.....	16
4	Tabulated data from empty test section test at $U_{ts} = 5$ m/s .....	17
5	Tabulated data from empty test section test at $U_{ts} = 10$ m/s .....	19
6	Tabulated data from empty test section test at $U_{ts} = 15$ m/s .....	21
7	Tabulated data from empty test section test at $U_{ts} = 20$ m/s .....	23
8	Tabulated data from empty test section test at $U_{ts} = 24.4$ m/s .....	25
9	Tabulated data from tests at $U_{ts} = 5$ m/s with the elevated ground plane installed .....	27
10	Tabulated data from tests at $U_{ts} = 10$ m/s with the elevated ground plane installed.....	29
11	Tabulated data from tests at $U_{ts} = 15$ m/s with the elevated ground plane installed.....	31
12	Tabulated data from tests at $U_{ts} = 20$ m/s with the elevated ground plane installed.....	33
13	Tabulated data from tests at $U_{ts} = 25$ m/s with the elevated ground plane installed.....	35

## Glossary

ADC	Analog to Digital Converter
DST	Defence Science and Technology
FS	Full Scale
LSWT	Low Speed Wind Tunnel
PS	Pitot-Static
RSS	Root-Sum-Square
RWT	Research Wind Tunnel
SCR	Sting Column Rig

## Notation

$C_0$	Constant term in linear regression analysis (Pa)
$K$	Calibration factor
$N$	Number of measured values
$\Delta P$	Static pressure differential (Pa)
$P_{ts}$	Test section absolute pressure (Pa)
$q_{ts}$	Test section dynamic pressure (Pa)
$R$	Universal gas constant for dry air, 287.04 kJ/kg·K
$Re_x$	Reynolds number based on dimension $x$
$T_{ts}$	Test section temperature (°C)
$U_{ts}$	Test section wind speed (m/s)
$x$	A linear dimension used in the calculation of $Re_x$ (m)

### Greek Symbols

$\mu_{ts}$	Test section air dynamic viscosity (Pa·s)
$\rho_{ts}$	Test section air density (kg/m <sup>3</sup> )

UNCLASSIFIED

DST-Group-TN-1728

*This page is intentionally blank*

UNCLASSIFIED

# 1. Introduction

The DST Group Research Wind Tunnel (RWT) test section dynamic pressure, from which the wind speed is calculated, has traditionally been measured by using a Pitot-static (PS) tube mounted in the test section. The PS tube is positioned near the aft end of the test section, such that it does not interfere with a test article. However, the dynamic pressure measurement is localised and cannot give an indication of the average wind speed in the test section, which is often used as a reference parameter in test calculations and data reduction.

The DST Low Speed Wind Tunnel (LSWT) has two piezo-rings, which are connected to pressure transducers, installed circumferentially before and after the contraction section. These rings measure the difference in static pressure between the two stations. This static pressure differential  $\Delta P$  is related to the dynamic pressure at some station downstream of the piezo-rings as per Eq. (1);

$$q_{ts} = K \Delta P, \quad (1)$$

where  $q_{ts}$  is the test section dynamic pressure and  $K$  is a calibration factor to be determined. This method of determining the test section dynamic pressure is outlined in greater detail by [1]. The advantage of this technique is that an intrusive measurement of dynamic pressure is not required once the calibration factor is obtained. Work has been done by [2] and [3] to obtain calibration factors for the LSWT at multiple centre-line locations in the test section. These factors are now used regularly in LSWT test programmes. [3] also obtained calibration factors in the LSWT test section when the Sting Column Rig (SCR) was installed. It was observed that the presence of the SCR had an appreciable influence on the calibration factor, which was attributed to tunnel blockage effects.

The RWT has pressure rings<sup>1</sup> installed similarly to the LSWT, in that they are placed before and after the contraction section. These pressure rings were never calibrated and thus have not been used in any tests to date. The cross-sectional shape of the RWT test section is geometrically similar to the LSWT, and both wind tunnels have the same contraction ratio. Thus, a similar calibration technique as that of [2] and [3] is carried out for the RWT pressure rings. However, [2] and [3] found that the calibration factor did not change significantly with stream-wise location inside the test section. Also, the RWT is not generally used for high fidelity testing, and the models usually do not span the length of the test section. Thus, calibration factors inside the RWT are obtained at one centre-line station only, for two cases:

1. Empty test section, and
2. An elevated ground plane (EGP) installed

The latter case is included because the findings of [3] suggested influence of model support blockage on the calibration factor.

---

<sup>1</sup>Pressure rings operate equivalently to piezo-rings in this context.

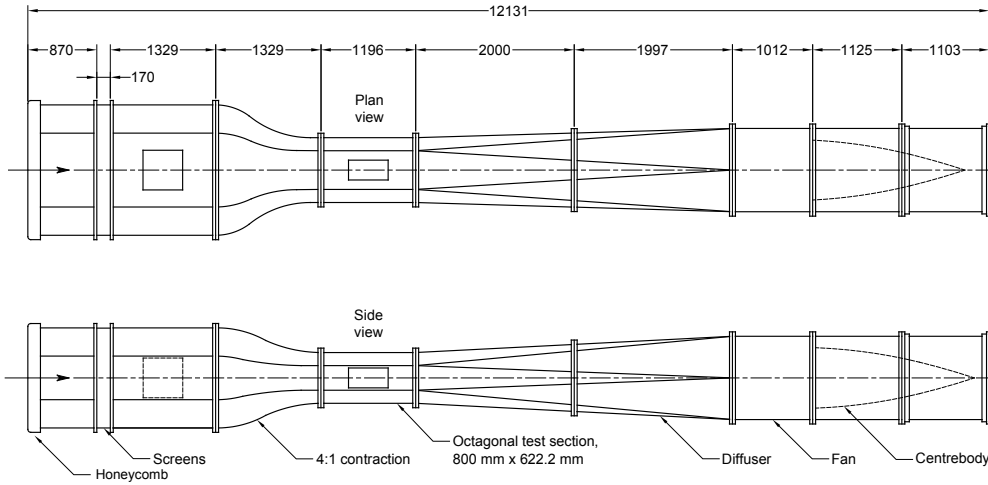


Figure 1: The DST Group Research Wind Tunnel. Diagram taken from [4].

## 2. Research Wind Tunnel Description

The DST RWT is a suction-type, closed-jet tunnel, with an open airflow return circuit. The flow is initially conditioned at the inlet using honeycomb screen with square cells, and subsequently with three turbulence reducing screens. A 4:1 contraction leads into the test section, which has an irregular-octagonal cross-section that is 800 mm wide, 622.2 mm high and 1196 mm long. The width and height test section dimensions are a scaled-down version of the LSWT by a linear factor of 3.429 [4]. The cross sectional area of the LSWT is 5.283 m<sup>2</sup>, so this gives a RWT test section cross-sectional area of 0.449 m<sup>2</sup>. A single-stage, twenty-four (24) blade fan, driven by a 22 kW AC motor, is downstream of the test section. The fan and motor permit a maximum wind speed of approximately 28 m/s with no turbulence reducing screens installed. With the three screens installed, the maximum achievable wind speed in the tunnel is around 25 m/s. Usually, the RWT would be used with the turbulence reducing screens installed, as a study by [4] found significant non-uniformity in flow angularity and turbulence intensities in the test section without the screens installed. At nominal wind speeds of 10–20 m/s with the screens installed, the turbulence intensities were below 0.3% and flow angularity was within 0.5° [4]. A diagrammatic representation of the RWT is shown in Fig. 1.

The tunnel coordinate system ( $x_T, y_T, z_T$ ) has its origin along the tunnel centre-line and at the entrance of the test section, with flow in the positive  $x_T$  direction and  $z_T$  is positive towards the tunnel floor. According to the right-hand rule, the  $y_T$  direction is then positive towards the starboard side of the tunnel, when viewing upstream (Fig. 2).

The RWT test section may accommodate a pressure tapped EGP that spans the entire width of the test section. The EGP was designed to interface with four aerodynamically shaped vertical struts, which offset the EGP from the test section floor. However, it was found when installing the EGP that there was no width tolerance between the EGP and the RWT test section walls, and instead the EGP was supported by the test section walls rather than the four struts (Fig. 3). The tight fit and mass of the EGP meant that dislodging or vibrations of the

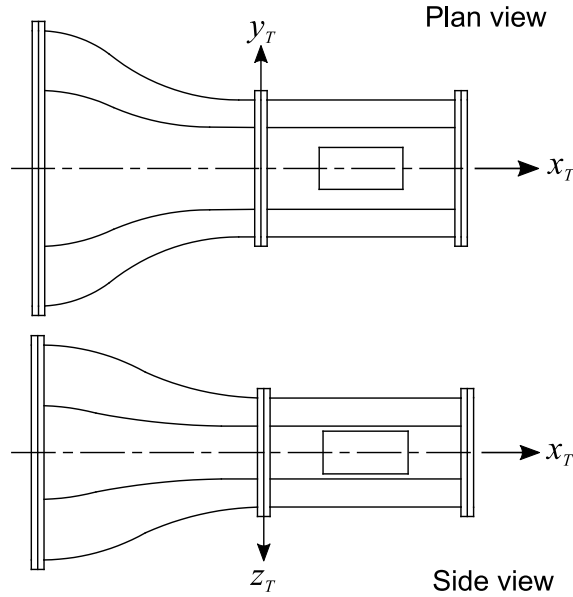


Figure 2: RWT coordinate system.

EGP did not occur, and the EGP sat level with the test section. Thus, instead of modifying the EGP such that mounting on the four struts was possible, the testing was conducted with the EGP supported by the test section walls. The EGP has a blockage ratio of approximately 3%, which is below the maximum recommended value of 7% in low-speed wind tunnel testing [1].

### 3. Test Equipment

An overview of all the testing instrumentation and connections used in the calibration is shown in Fig. 5. A NI 9215 ADC module was used to sample all the measurement instrumentation voltages. The NI 9215 has an expanded bias uncertainty in voltage measurements at 95% confidence of  $\pm 0.18 \text{ mV}^2$ .

#### 3.1. Pitot-Static Probe

A United Sensor straight PS tube (S/N MC 1148) with a tip diameter of 1.55 mm was used for providing a measure of  $q_{ts}$ . The PS tube was interfaced with a sting (Fig. 4), which was guyed with wire to minimise deflections, and positioned on the centre-line of the RWT test section as per Fig. 5. It was estimated that the PS tube longitudinal axis was aligned with the mean flow direction to within  $\pm 2^\circ$ .

During the tests, the sting was observed to undergo small amplitude (of order 2 mm or less) oscillations, at the higher wind speeds ( $> 15 \text{ m/s}$ ) despite the guying. The frequency of these

<sup>2</sup>The author has determined these values from separate calibration tests.

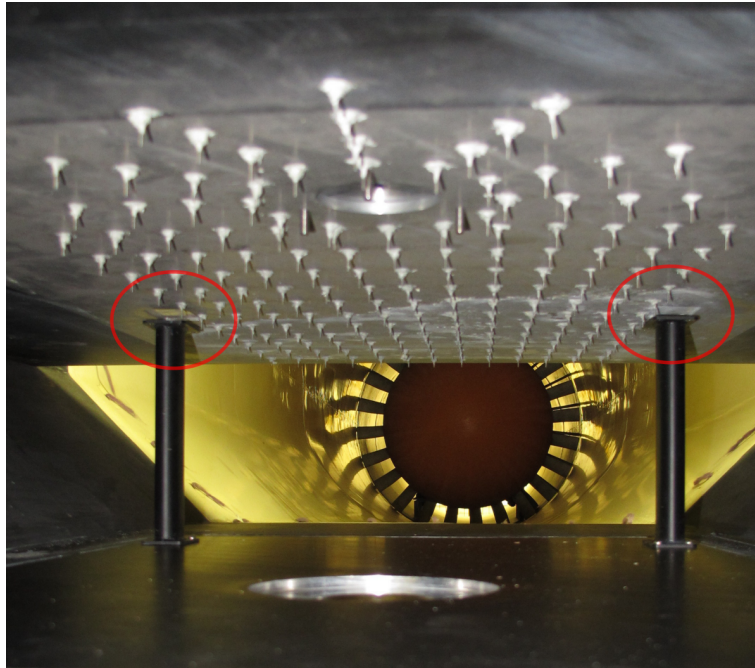


*Figure 3: The elevated ground plane supported by the test section walls rather than the vertical struts, as highlighted by the red ellipses in the image. Note that the mean flow direction is into the page, and only the two aft struts may be seen in this photograph.*



(i)



(ii)

*Figure 4: Photographs of the pitot-static tube fixed to the sting mount inside the RWT for (i) an empty test section, and (ii) with the elevated ground plane installed.*

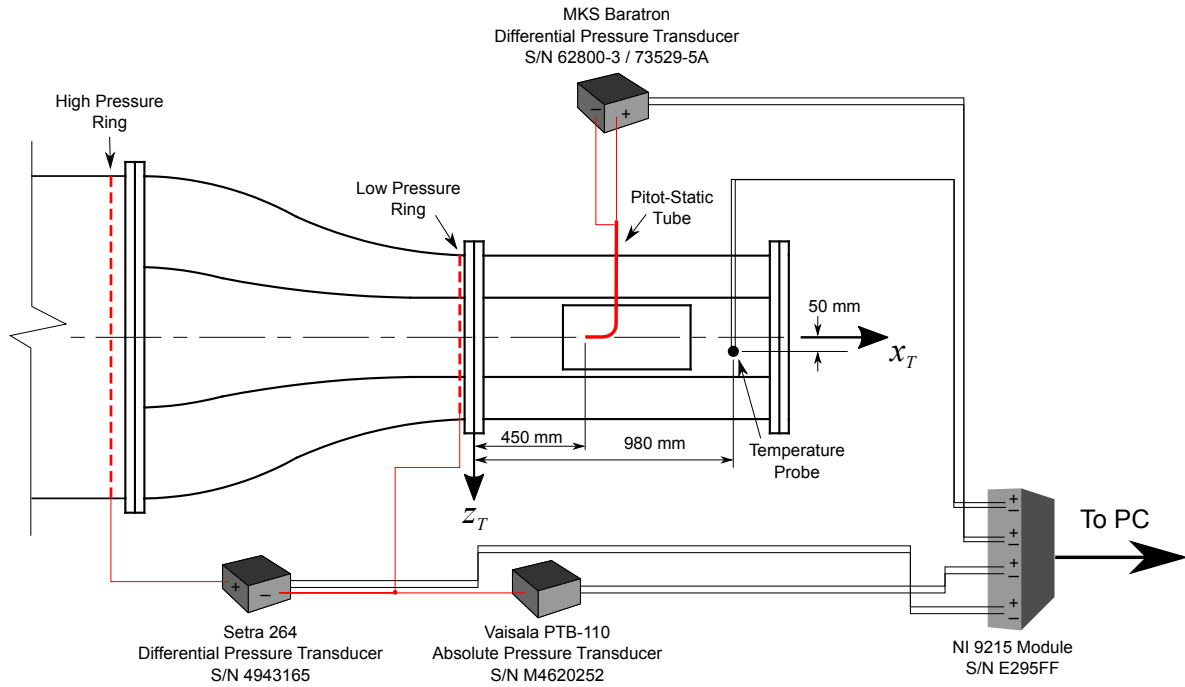


Figure 5: The instrumentation used, along with pneumatic (—) and electrical (—) connections. Note that the schematic is not to scale, and that flow is in the positive  $x_T$  direction. The PS tube was installed at  $y_T = 0$ .

oscillations were much greater than the data output frequency of  $q_{ts}$  (Section 4), thus it was anticipated that the oscillations would not significantly affect the time averaged measurements.

### 3.2. Pressure Transducers

Each pressure ring consist of four evenly spaced tappings installed circumferentially about the RWT. The high and low pressure rings are connected respectively to the positive and negative inputs of a Setra 264 differential pressure transducer (S/N 4943165) to measure  $\Delta P$ . The low pressure ring is also connected to a Vaisala PTB110 absolute pressure transducer (S/N M4620252) to measure the absolute static pressure at the entrance to the test section  $P_{ts}$ . The PS tube is connected to an MKS Baratron differential pressure transducer (S/N 62800-3/73529-5A) to measure  $q_{ts}$ .

### 3.3. Temperature Probe

A LabJack EI-1034 temperature probe installed near the aft end of the test section is used to measure the test section temperature  $T_{ts}$ . This value is used, along with the absolute pressure measured by the Vaisala transducer (Section 3.2), to calculate test section air density  $\rho_{ts}$  as;

$$\rho_{ts} = \frac{P_{ts}}{RT_{ts}}, \quad (2)$$

where  $R$  is the universal gas constant for dry air, equal to 287.04 kJ/kg·K.

## 4. Test Methodology

The test matrix is displayed in Table 1. The PS tube was used to set the nominal test section wind speed  $U_{ts}$ , according to;

$$U_{ts} = \sqrt{\frac{2q_{ts}}{\rho_{ts}}}. \quad (3)$$

The testing order of  $U_{ts}$  was randomised to prevent any nuisance variable from affecting the results. Each  $U_{ts}$  set point was assigned an integer ranging from 1 to 5, corresponding to 5, 10, 15, 20 and 25 m/s respectively, and a random sequence generator utilising atmospheric noise [5] was used to generate  $U_{ts}$  sequences for each run. One replicate for each test section configuration was performed in order to confirm repeatability of the data. The  $U_{ts}$  set points for the replicate tests were also randomised using the random sequence generator. The position of the PS tube as displayed in Fig. 5 did not change throughout the testing. The stream-wise position of the PS tube was  $x_T = 450$  mm, or 37% of the test section length; this station was chosen as a good representation of the wind speed near the entrance of the test section, and also potential model installation locations.

At each  $U_{ts}$  set point, two user-written LabVIEW<sup>®</sup> programs were used in the following way:

1. A program called ‘‘RWT Wind Speed Indicator - Baratron.vi’’ samples the Baratron, Vaisala and temperature probe in order to calculate  $U_{ts}$  using Eqs. (2) and (3) with the PS tube positioned as shown in Fig. 5.
2. Once the  $U_{ts}$  set point is achieved, ‘‘RWT Wind Speed Indicator - Baratron.vi’’ must be halted<sup>3</sup> and a program called ‘‘RWT Pressure Ring Calibration.vi’’ is executed, which samples the Setra 264 and the Baratron simultaneously, and logs the data.

Voltage data from the Setra 264 and Baratron were sampled continuously with an average of 1,000 samples taken at a sampling rate of 1,000 Hz, so that averaged voltage data was logged at 1 Hz. For each run, the voltage data were logged for a total period of 60 seconds. This gave a total of 60 samples from both the Setra 264 and the Baratron, for each test point. The 60 samples were then averaged again in post-processing to give a mean value of  $\Delta P$  and  $q_{ts}$  at each  $U_{ts}$  set point.

---

<sup>3</sup>This is because the NI 9215 module cannot run more than one task – or program, simultaneously.

Table 1: Pressure ring calibration test matrix.

Test Section Configuration	Run	$U_{ts}$ in Descending Order (m/s)
Empty	Baseline	5
		20
		25 <sup>a</sup>
		15
		10
	Replicate 1	20
		10
		15
		25 <sup>a</sup>
		5
EGP Installed	Baseline	5
		20
		15
		10
		25
	Replicate 1	10
		25
		15
		20
		5

<sup>a</sup> The reading at maximum fan power was 24.4 m/s.

## 5. Data Reduction

In general, the test section dynamic pressure  $q_{ts}$  is directly related to the change in static pressure across the two pressure rings  $\Delta P$  through the following equation;

$$q_{ts} = K\Delta P + C_0 \quad (4)$$

where  $C_0$  is the zero, or offset term. Here, the offset term is always zero since it was ensured before the tests that when  $q_{ts} = 0$ ,  $\Delta P = 0$ . Thus, Eq. (4) reduces to Eq. (1) and  $K$  may be determined through least-squares regression analysis from a set of  $N$  measured  $q_{ts}$  and  $\Delta P$  values as;

$$K = \frac{\sum_{i=1}^N (\Delta P)_i (q_{ts})_i}{\sum_{i=1}^N (\Delta P)_i^2} \quad (5)$$

Eq. (5) is closed loop and in standard texts, e.g. [6], the data points can be weighted to adjust for uncertainties in the “dependent” variable –  $q_{ts}$  in this case. However,  $q_{ts}$  is not strictly dependent on  $\Delta P$ , but like  $\Delta P$  is a *measured* quantity. Moreover, uncertainties exist not only in  $q_{ts}$  but also in the measurement of  $\Delta P$ . Thus, it is more appropriate to utilise a least-squares regression algorithm that accounts for uncertainties in both  $q_{ts}$  and  $\Delta P$ , to determine the values of and uncertainty in  $K$ . This process is not closed loop, and requires an iterative approach. In [7], such an iterative algorithm was developed; this procedure is used with the number of measured samples,  $N = 5$ , corresponding to each  $U_{ts}$  set point.

The standard error in the estimation of  $q_{ts}$  using the calculated  $K$  factors is given by;

$$SE = \sqrt{\frac{\sum_{m=1}^N (q_{ts_m} - \hat{q}_{ts_m})^2}{N - 1}}, \quad (6)$$

where  $q_{ts}$  is the measured test section dynamic pressure using the PS tube, and  $\hat{q}_{ts}$  is the back-calculated test section dynamic pressure according to Eq. (1).

Table 2: The value and expanded uncertainty at 95% confidence of the calibration factor  $K$  for each RWT test section configuration as determined using the least-squares method of [7], as well as the standard error of  $q_{ts}$  estimation.

Test Section Configuration	Run	Run Calibration Factor, $K$	Final Calibration Factor, $K$	Standard Error of $q_{ts}$ Estimation (Pa)
Empty	Baseline	$1.0934 \pm 0.0070$	$1.0931 \pm 0.0074$	0.83
	Replicate 1	$1.0928 \pm 0.0078$		
EGP installed	Baseline	$1.1639 \pm 0.0062$	$1.1642 \pm 0.0078$	1.06
	Replicate 1	$1.1644 \pm 0.0084$		

## 6. Results and Discussion

The results for the empty test section are shown in Fig. 6, and for the EGP installed in the test section in Fig. 7. Tabulated test data for the empty test section and with the EGP installed are included in Appendices B and C respectively. The final calibration factors  $K$  for the empty test section and with the EGP installed were the average of the baseline and replicate results. Expanded uncertainties in  $K$  are reported at 95% confidence with a coverage factor of 2. The final calibration factors for each test section configuration, along with the standard error of estimation, are tabulated in Table 2. The system uncertainties are summarised in Appendix A.

$K$  for the empty test section is similar to those obtained by [2] and [3] ( $\approx 1.07$ ) in the LSWT at a stream-wise station 21% of the test section length. The similarity in  $K$  values between the LSWT tests and the RWT tests could be because of the same contraction ratio, and test-section cross-sectional shape between the RWT and LSWT. The main differences between the study in the RWT and studies by [2] and [3] in the LSWT are:

1. The RWT contraction and test section are smaller than the ones in the LSWT, albeit by a constant scaling factor (Section 2). This could mean that flow viscous effects influence the value of  $K$ .
2. The RWT is an open circuit, suction configuration where the static pressure inside the test section is sub-atmospheric; the LSWT is closed circuit and operates nominally at atmospheric pressure.
3. The RWT flow conditioning upstream of the settling chamber comprises of square celled honeycomb and three turbulence reducing screens; the LSWT flow conditioning comprises only of triangular celled honeycomb.

It is outside the scope of this calibration to quantify the effects of these differences on the values of  $K$ . Furthermore, uncertainties in  $K$  were not reported for either study in the LSWT, so it is difficult to conclude that the observed difference in  $K$  between the RWT and LSWT is due to the aforementioned differences, and not simply within the uncertainty bounds of measurement. However, a brief discussion on each of the identified differences is presented.

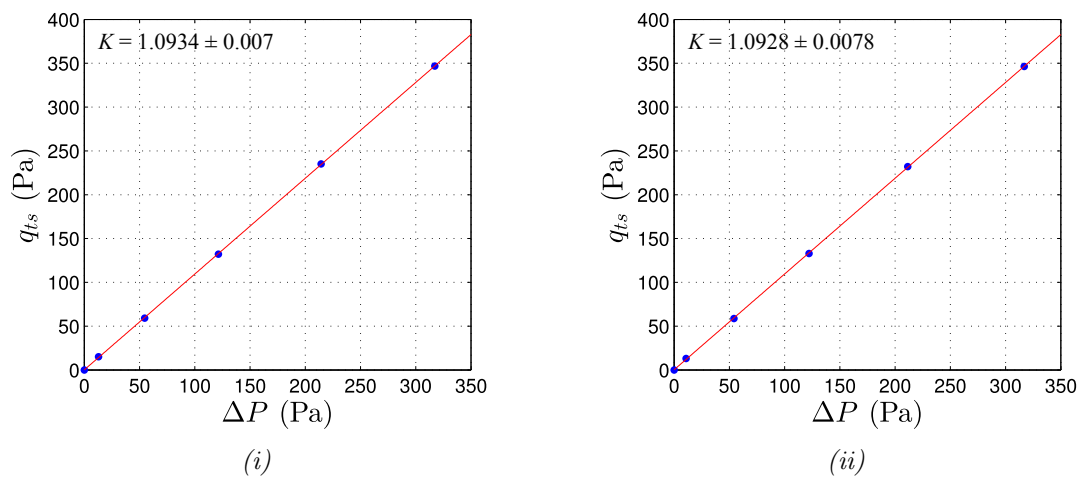


Figure 6: Least-squares regression fits (—) on empty test section data (●) for (i) baseline and (ii) replicate runs. The expanded uncertainty in the calibration factor  $K$  is also shown at 95% confidence with a coverage factor of 2.

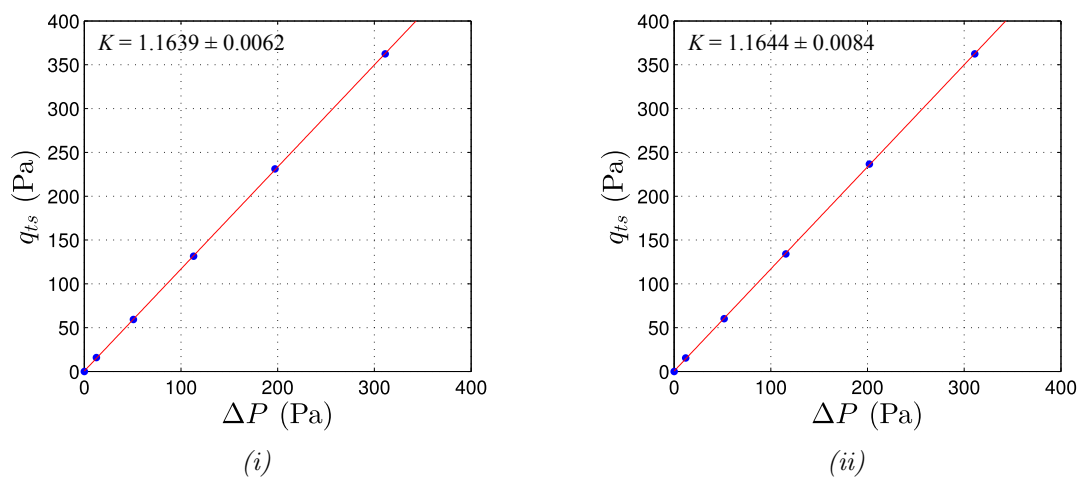


Figure 7: Least-squares regression fits (—) on elevated ground plane data (●) for (i) baseline and (ii) replicate runs. The expanded uncertainty in the calibration factor  $K$  is also shown at 95% confidence with a coverage factor of 2.

The Reynolds number  $Re_x$ , based on some internal dimension  $x$  of the wind tunnel test section, is defined as:

$$Re_x = \frac{\rho_{ts} U_{ts} x}{\mu_{ts}}, \quad (7)$$

where  $\mu_{ts}$  is the dynamic viscosity of the air in the test section. The LSWT calibrations by [2] and [3] were conducted over a range in  $U_{ts}$  of 5 to 90 m/s, at 5 m/s intervals. This covers the range in  $U_{ts}$  tested in the RWT. However, despite the same nominal wind speeds being tested between the LSWT and RWT, the values of  $Re_x$  will differ approximately by a factor of order  $O(3.4)$ , which is the scaling factor between the sizes of the RWT and LSWT contraction and test sections (Section 2). It is well known that the boundary layer characteristics for internal flows are strongly dependent on the Reynolds number, and it could be that this difference in  $Re_x$  between the RWT and LSWT is contributing to the observed difference in  $K$ .

Upon inspection of Eqs. (2) and (7), which shows the dependency of  $Re_x$  on  $\rho_{ts}$ , operating at sub-atmospheric pressure in the RWT as opposed to atmospheric pressure in the LSWT means that differences in  $Re_x$  could occur. However, the variation of  $\rho_{ts}$  across the tested range was no more than 1%<sup>4</sup>, which translates to an effectively negligible change in  $Re_x$ . Also, the values of  $q_{ts}$  and  $\Delta P$  are obtained through differential measurements, inherently negating the effect of changes in absolute pressure.

The difference in flow conditioning between the RWT and LSWT theoretically should not affect the difference in observed  $K$  values. The derivation of Eq. 1 from the Bernoulli equation (refer to [1, chap. 6]) considers only the flow between the pressure rings and into the test section. It does not account for the upstream flow state or upstream losses associated with flow conditioning devices. The upstream flow is effectively an “inlet” condition to the pressure rings. However, in practice, changing the flow conditioning is likely to cause differences in the flow uniformity across the test section, see [4]. If the position of the PS tube remains fixed, and the flow conditioning is changed in a given wind tunnel, it may be that the calibration factor is slightly different, owing to changes in flow uniformity. Nevertheless, the difference in flow conditioning between the RWT and LSWT likely does not significantly affect the observed difference in  $K$ .

$K$  for the case where the EGP was installed increased significantly from the empty test section value. This is opposite to what [3] observed when the SCR was installed in the LSWT, where the value of  $K$  decreased slightly compared to the empty test section. It was observed here that the maximum wind speed as determined using the PS tube was slightly greater when the EGP was installed ( $U_{ts} = 25$  m/s), than with the empty test section ( $U_{ts} = 24.4$  m/s). This is due to the blockage caused by the EGP. Continuity laws govern that the 3% blockage should cause a 3% increase in  $U_{ts}$ ; this is in fact what is observed when the EGP is removed from the test section,

$$24.4 \text{ m/s} \times 1.03 \text{ (blockage)} \approx 25 \text{ m/s.}$$

---

<sup>4</sup> $\rho_{ts}$  can also change due to variations in test section temperature.

However, the increase in  $K$  for when the EGP is installed is directly associated with a decrease in  $\Delta P$  for a set  $q_{ts}$  (Eq. 1). This means that the static pressure differential between the high and low pressure ring has decreased. Though not conclusive, this might be explained by the blockage induced by the EGP: the region in front of the EGP contains dividing streamlines that terminate as stagnation points on the EGP leading edges. In the stagnation regions, the static pressure is comparatively higher than what it would be in the absence of stagnation regions (i.e. no EGP installed). These relatively high pressure regions extend upstream by some distance and it is possible that the low pressure ring is influenced by these high pressure regions. It is difficult to compare directly with the measurements in [3], since the PS tube in that work was placed in front of the SCR on the LSWT centre-line, and uncertainties in  $K$  were not reported.

The calibration factors obtained here should be used to calculate the reference wind speed in the RWT. Installation of test articles will likely change the calibration factor due to blockage, but this effect may be corrected if necessary. Removing the RWT turbulence screens is also likely to change the calibration factor. As recommended in [4], the RWT should not be used without the turbulence screens.

## 7. References

- [1] Barlow, J., Rae, W. & Pope, A. (1999) *Low-Speed Wind Tunnel Testing*, 3rd edn, John Wiley & Sons Inc., New York.
- [2] Edwards, C. D. (2000) *Calibration of the Reference Velocity in the Test Section of the Low Speed Wind Tunnel at the Aeronautical and Maritime Research Laboratory*, Technical Note DSTO-TN-0248, Aerospace Division, DST Group.
- [3] Lam, S. (2015) *Calibration of the DST Group Low Speed Wind Tunnel Test-Section Reference Velocity*, Draft Report.
- [4] Erm, L. P. & Jacquemin, P. P. E. (2015) *Calibration of the Flow in the Test Section of the Research Wind Tunnel at DST Group*, Technical Note DSTO-TN-1468, Aerospace Division, DST Group.
- [5] [www.random.org](http://www.random.org) (2017) Random Number Generator, URL.
- [6] Bevington, P. R. (1969) *Data Reduction and Error Analysis for the Physical Sciences*, McGraw-Hill, New York.
- [7] Reed, B. C. (2010) A spreadsheet for linear least-squares fitting with errors in both coordinates, *Phys. Educ.*
- [8] AIAA (1999) Assessment of experimental uncertainty with application to wind tunnel testing, Standard No. AIAA S-071A.
- [9] Setra Systems (2011) *Setra Model 264 Calibration Certificate*, Calibration Report 24010930, Setra Systems, Inc, 159 Swanson Road, Boxborough, MA 01719, USA.
- [10] Howes, M. (2017) *Measurement Report on Pressure Transducer, MKS model 220CD-00100A2B / PDR-C-1C serial number 62800-3 / 73529-5A*, Calibration Report No. RN170560, National Measurement Institute, 36 Bradfield Road, West Lindfield, NSW 2070, Australia.
- [11] Vaisala (2016) *PTB110 Barometer Calibration Certificate*, Calibration Report H47-16460020, Vaisala Oyj, PO Box 26, FI-00421 Helsinki, Finland.
- [12] [www.labjack.com](http://www.labjack.com) (2017) EI-1034 Datasheet, URL.

UNCLASSIFIED

DST-Group-TN-1728

*This page is intentionally blank*

UNCLASSIFIED

## Appendix A. System Uncertainties

System uncertainties are calculated according to the methodology outlined in [8] and summarised in Table 3. Bias uncertainty in instrumentation was estimated from calibration data and includes the NI 9215 uncertainty in voltage measurements. Bias uncertainty in  $K$  was determined using the method of [7]. Precision uncertainty in instrumentation was estimated using the standard deviation of 60 samples at each  $U_{ts}$  set point, with precision uncertainty over all wind speeds calculated as the Root-Sum-Square (RSS) of the precision uncertainty at each  $U_{ts}$  set point. It was assumed that precision uncertainty in  $K$  was negligible.

The Setra 264 differential pressure transducer was factory calibrated in December 2011 and has a standard bias uncertainty of  $\pm 0.25\%$  FS, or  $\pm 1.56$  Pa [9]. The MKS Baratron differential pressure transducer was last calibrated in June 2017 and has an expanded bias uncertainty of  $\pm 0.15$  Pa at 95% confidence with a coverage factor of 2 [10]. The Vaisala absolute pressure transducer and temperature probe used to calculate  $U_{ts}$  were not logged during the calibration, so precision uncertainties in these instruments could not be estimated. The Vaisala was last calibrated in November 2016 and has an expanded bias uncertainty of  $\pm 15$  Pa at 95% confidence with a coverage factor of 2 [11]. The temperature probe has a standard bias uncertainty of  $\pm 0.22$  °C [12].

Table 3: Test uncertainties

Parameter	Test Section Configuration	Bias Uncertainty	Precision Uncertainty	Expanded Uncertainty 95% Confidence Coverage factor = 2
$\Delta P$ (Pa)	Empty	1.56	0.189	3.14
	EGP		0.172	3.13
$q_{ts}$ (Pa)	Empty	0.13	0.235	0.537
	EGP		0.198	0.474
$K$	Empty	0.0037	–	0.0074
	EGP	0.0039	–	0.0078
$P_{ts}$ (Pa)	Empty	7.5	–	15
	EGP		–	
$T_{ts}$ (°C)	Empty	0.22	–	0.44
	EGP		–	

## Appendix B. Tabulated Empty Test Section Data

Table 4: Tabulated data from empty test section test at  $U_{ts} = 5$  m/s

Time (s)	Baseline $q_{ts}$	Baseline $\Delta P$	Repeat $q_{ts}$	Repeat $\Delta P$
0	15.083	12.904	14.716	12.223
1	15.095	12.872	14.584	12.280
2	15.031	12.894	14.385	12.210
3	14.864	12.887	14.136	12.126
4	15.136	12.975	13.974	12.054
5	15.393	12.982	14.463	12.044
6	15.209	12.812	14.580	11.920
7	15.067	12.836	14.723	11.461
8	15.062	12.933	14.348	11.068
9	15.074	12.906	13.421	10.689
10	15.240	12.895	12.840	10.794
11	15.314	12.867	12.561	10.883
12	15.338	12.947	12.443	10.870
13	15.023	12.933	12.707	10.769
14	15.018	12.846	13.069	10.690
15	15.161	12.799	13.299	10.687
16	14.929	12.829	13.287	10.568
17	15.314	12.867	12.750	10.562
18	15.860	12.801	12.636	10.776
19	15.831	12.883	12.383	10.992
20	15.472	12.996	12.738	11.008
21	15.087	13.070	13.188	10.932
22	14.537	13.027	13.080	11.180
23	14.918	12.994	13.061	11.137
24	15.633	12.944	12.891	11.096
25	15.695	12.917	13.135	11.008
26	15.020	12.953	13.063	10.843
27	14.525	12.893	13.161	10.562
28	14.462	12.865	12.970	10.709
29	15.042	12.968	13.003	10.778
30	15.246	12.916	12.994	10.745
31	15.345	12.943	13.210	10.792
32	15.249	12.818	13.099	10.677
33	15.155	12.656	13.274	10.542
34	14.589	12.756	13.108	10.434
35	15.350	12.762	12.803	10.292
36	15.774	12.871	12.846	10.289
37	15.785	12.956	12.677	10.301
38	15.086	13.080	12.843	10.193
39	15.287	13.023	12.603	10.122

UNCLASSIFIED

DST-Group-TN-1728

Table 4 Continued: Tabulated data from empty test section test at 5 m/s

---

40	15.178	12.993	12.474	10.182
41	14.905	12.812	12.215	10.346
42	14.783	12.836	12.362	10.505
43	15.009	12.989	12.780	10.580
44	15.361	13.045	12.939	10.650
45	15.412	12.957	12.974	10.675
46	15.503	12.936	12.904	10.502
47	15.217	12.923	12.693	10.518
48	14.930	12.991	12.546	10.399
49	15.078	12.985	12.694	10.217
50	15.530	12.910	12.645	10.327
51	15.687	12.932	12.902	10.376
52	15.454	12.991	12.673	10.371
53	15.222	12.907	12.509	10.449
54	14.794	12.959	12.545	10.667
55	14.588	12.939	12.995	10.847
56	14.573	12.821	13.024	10.955
57	14.630	12.741	13.235	11.174
58	14.424	12.721	13.444	11.405
59	14.891	12.832	13.690	11.618
60	15.261	12.952	13.902	11.483

---

UNCLASSIFIED

Table 5: Tabulated data from empty test section test at  $U_{ts} = 10$  m/s

Time (s)	Baseline $q_{ts}$	Baseline $\Delta P$	Repeat $q_{ts}$	Repeat $\Delta P$
0	59.381	54.801	59.604	55.244
1	59.189	54.738	60.061	54.809
2	59.199	54.630	59.731	54.255
3	59.342	54.536	58.848	54.456
4	58.982	54.331	58.796	54.435
5	58.657	54.434	58.574	54.315
6	58.959	54.346	58.390	54.296
7	59.017	54.421	58.606	53.953
8	59.074	54.509	58.430	54.055
9	59.123	54.391	58.468	54.249
10	58.957	54.529	58.784	54.531
11	58.975	54.710	59.160	54.540
12	59.188	54.345	59.156	54.560
13	59.164	54.288	59.277	54.650
14	58.797	54.602	59.394	54.623
15	58.895	54.588	59.006	54.209
16	58.992	54.438	58.776	54.287
17	59.021	54.815	58.732	54.416
18	59.268	54.732	58.947	54.648
19	59.270	54.420	59.322	54.600
20	59.226	54.582	59.286	54.379
21	58.780	54.902	59.175	54.358
22	59.051	54.573	59.100	54.534
23	58.795	54.580	59.166	54.637
24	59.110	54.489	59.529	54.273
25	59.163	54.801	58.901	54.025
26	59.211	54.917	58.334	53.884
27	59.648	55.039	58.440	54.007
28	59.616	54.889	58.472	53.823
29	59.475	54.541	58.557	53.897
30	59.236	54.591	58.699	53.728
31	59.441	54.593	58.314	53.760
32	59.125	54.329	58.423	53.606
33	58.893	54.178	58.480	53.710
34	58.766	54.375	58.441	53.867
35	59.007	54.280	58.511	53.773
36	58.765	54.226	58.749	54.061
37	58.750	54.652	58.617	53.998
38	58.932	54.780	58.429	53.755
39	59.184	54.720	58.201	53.880
40	59.278	54.684	58.028	54.202

UNCLASSIFIED

DST-Group-TN-1728

Table 5 Continued: Tabulated data from empty test section test at 10 m/s

---

41	59.362	54.749	58.241	54.108
42	59.071	54.668	58.300	53.832
43	59.369	54.717	57.953	54.078
44	59.419	54.636	58.060	54.184
45	59.547	54.806	57.997	54.279
46	59.435	54.989	58.372	54.477
47	59.579	54.945	58.991	54.451
48	59.593	54.773	59.073	54.625
49	59.401	54.923	59.200	54.787
50	59.127	54.996	59.188	54.254
51	58.686	54.884	58.697	54.121
52	58.116	54.845	58.577	53.859
53	58.694	54.656	58.483	53.840
54	59.360	54.675	58.207	53.648
55	59.785	54.589	58.223	53.904
56	59.841	54.666	58.362	54.022
57	59.779	54.736	58.502	54.000
58	59.336	54.752	58.260	53.741
59	59.177	54.662	58.235	53.685
60	59.239	54.583	57.892	53.866

---

UNCLASSIFIED

Table 6: Tabulated data from empty test section test at  $U_{ts} = 15$  m/s

Time (s)	Baseline $q_{ts}$	Baseline $\Delta P$	Repeat $q_{ts}$	Repeat $\Delta P$
0	132.856	120.964	133.502	121.955
1	132.539	121.450	133.375	121.923
2	132.280	121.572	133.278	122.130
3	132.331	121.432	133.027	122.088
4	132.156	120.778	132.666	122.484
5	131.894	120.819	132.877	122.538
6	132.026	121.410	132.645	122.054
7	131.469	121.572	132.876	122.476
8	131.218	121.427	133.000	122.509
9	131.487	121.550	133.097	122.345
10	132.367	121.187	132.913	122.358
11	132.163	121.130	132.962	122.126
12	132.086	121.265	133.130	121.808
13	131.745	121.487	132.824	121.628
14	131.432	121.613	132.858	122.280
15	132.465	121.786	132.861	122.009
16	132.532	121.626	132.714	122.009
17	132.192	121.544	132.526	121.910
18	132.079	121.299	132.783	121.938
19	132.119	121.688	132.875	122.230
20	132.691	121.604	132.869	122.133
21	132.887	121.336	132.793	122.319
22	132.582	121.481	132.714	122.089
23	132.412	121.443	132.855	122.079
24	131.747	121.363	132.760	121.990
25	131.821	121.454	132.621	122.057
26	131.770	121.121	132.951	122.075
27	131.545	121.409	133.202	122.397
28	131.385	121.273	133.315	122.542
29	131.642	121.194	134.013	122.657
30	131.918	121.642	133.823	122.292
31	132.171	121.299	133.769	122.533
32	132.050	121.238	133.573	122.185
33	132.334	121.382	132.978	122.433
34	132.293	121.458	132.533	122.016
35	132.203	121.417	132.403	121.987
36	132.333	121.362	132.358	122.063
37	132.478	121.417	132.556	122.194
38	132.479	120.833	132.864	121.937
39	132.219	121.427	133.010	122.051
40	132.192	121.298	132.981	122.186

UNCLASSIFIED

DST-Group-TN-1728

Table 6 Continued: Tabulated data from empty test section test at 15 m/s

---

41	131.709	121.266	133.061	122.224
42	131.690	121.556	133.151	122.069
43	131.679	121.511	132.830	122.086
44	131.774	121.075	132.878	122.020
45	132.323	121.530	132.591	121.821
46	132.620	121.040	132.500	122.030
47	132.403	121.218	132.741	122.302
48	132.416	121.502	132.873	122.077
49	132.298	121.541	132.943	121.932
50	132.276	121.559	132.732	121.924
51	132.689	121.256	132.888	121.940
52	132.825	120.942	133.105	122.322
53	131.735	121.173	133.217	121.966
54	130.901	121.343	133.118	121.953
55	131.438	121.500	132.903	122.151
56	131.505	121.379	132.727	122.176
57	131.827	121.156	132.768	121.890
58	132.144	121.430	132.815	121.757
59	132.012	121.042	132.337	121.702
60	131.864	120.979	132.619	122.138

---

UNCLASSIFIED

Table 7: Tabulated data from empty test section test at  $U_{ts} = 20$  m/s

Time (s)	Baseline $q_{ts}$	Baseline $\Delta P$	Repeat $q_{ts}$	Repeat $\Delta P$
0	234.556	214.127	231.057	210.796
1	234.625	214.564	231.109	210.570
2	234.605	214.449	230.997	211.298
3	234.725	213.989	231.722	211.072
4	234.619	213.891	231.792	210.930
5	234.686	213.764	231.402	210.300
6	234.407	213.289	230.682	210.191
7	234.586	213.231	229.924	209.876
8	234.625	212.930	230.021	210.046
9	234.010	212.287	230.442	210.318
10	233.278	212.445	230.490	210.804
11	233.359	212.508	231.283	211.125
12	232.983	212.948	232.107	211.212
13	233.320	213.407	232.415	211.338
14	233.979	213.592	232.231	210.736
15	234.180	213.580	231.304	210.835
16	234.557	214.394	231.412	210.900
17	234.797	213.785	232.206	211.290
18	234.887	214.535	232.381	211.948
19	235.256	213.808	232.627	212.010
20	234.472	212.706	232.772	211.743
21	233.522	212.391	232.655	211.459
22	233.240	213.077	232.183	211.663
23	234.044	213.572	232.110	211.874
24	234.379	214.417	232.152	211.662
25	235.120	214.768	231.793	211.350
26	235.687	214.950	231.410	211.687
27	235.864	215.111	231.845	211.551
28	236.078	215.146	232.446	211.612
29	236.209	214.712	232.728	211.624
30	235.558	214.668	232.503	211.396
31	235.117	214.437	232.053	211.382
32	235.052	214.785	231.899	211.530
33	235.220	214.274	232.026	211.237
34	235.248	214.583	232.112	211.575
35	235.213	214.002	232.381	211.517
36	234.592	214.254	232.009	210.846
37	234.722	214.579	231.045	210.852
38	235.213	214.342	231.568	211.323
39	235.203	214.570	232.073	210.843
40	235.515	214.692	231.962	210.738

UNCLASSIFIED

DST-Group-TN-1728

Table 7 Continued: Tabulated data from empty test section test at 20 m/s

---

41	235.460	214.621	231.740	210.357
42	235.925	214.526	231.328	209.846
43	235.681	214.761	231.740	210.740
44	235.734	214.575	232.094	212.019
45	236.162	214.856	233.177	212.193
46	236.074	214.920	233.295	212.678
47	236.261	215.152	233.714	212.793
48	235.913	215.255	233.870	212.647
49	235.757	215.214	233.094	212.113
50	235.648	214.804	232.893	211.796
51	235.427	215.302	232.514	211.711
52	235.773	215.211	232.353	212.219
53	236.168	215.928	232.434	212.493
54	236.562	215.380	232.622	212.004
55	236.705	215.857	232.444	211.814
56	237.020	215.746	232.790	212.302
57	237.249	215.623	232.958	212.513
58	236.526	215.693	233.492	211.542
59	236.602	215.542	233.010	211.963
60	235.950	215.808	232.906	212.169

---

UNCLASSIFIED

Table 8: Tabulated data from empty test section test at  $U_{ts} = 24.4$  m/s

Time (s)	Baseline $q_{ts}$	Baseline $\Delta P$	Repeat $q_{ts}$	Repeat $\Delta P$
0	347.729	316.861	346.276	317.151
1	347.350	317.121	346.668	317.423
2	347.414	317.354	346.766	317.177
3	347.096	317.272	346.916	317.296
4	346.829	316.987	346.397	316.952
5	346.096	317.431	346.199	316.836
6	346.667	317.079	346.514	317.007
7	346.387	317.461	346.295	317.314
8	347.093	317.318	346.268	317.015
9	347.058	317.577	346.694	316.896
10	347.845	317.654	347.410	317.561
11	347.661	317.329	347.125	317.057
12	347.592	317.383	346.463	317.208
13	347.180	317.641	346.388	316.826
14	347.304	317.369	346.284	316.945
15	347.260	317.092	346.905	316.948
16	347.039	316.740	347.240	316.989
17	346.505	317.334	346.775	316.829
18	346.580	317.806	346.833	317.271
19	347.179	317.476	347.143	316.783
20	347.284	317.263	346.677	316.497
21	347.413	317.069	346.449	316.623
22	347.411	317.050	346.638	316.928
23	347.266	317.114	346.912	316.882
24	346.657	317.519	346.404	316.411
25	346.650	317.177	345.709	316.530
26	346.350	317.354	346.291	316.681
27	346.358	317.439	346.341	317.016
28	346.693	317.347	347.004	316.809
29	346.850	317.094	346.352	317.042
30	347.445	317.252	346.073	316.815
31	347.590	317.405	345.869	316.824
32	347.601	317.109	346.252	316.810
33	347.400	317.070	345.912	316.175
34	346.654	317.184	345.756	316.650
35	346.287	316.995	345.904	316.914
36	345.933	317.145	345.760	316.362
37	346.327	317.028	345.485	316.562
38	346.063	316.977	345.832	317.195
39	346.184	317.353	346.396	316.520
40	346.878	317.430	346.905	316.528

UNCLASSIFIED

DST-Group-TN-1728

Table 8 Continued: Tabulated data from empty test section test at 24-4 m/s

---

41	347.682	317.575	346.356	316.404
42	347.677	317.067	346.157	316.461
43	347.106	316.646	347.158	317.136
44	346.111	316.684	347.245	316.791
45	345.903	316.610	346.899	316.808
46	346.845	317.429	346.055	316.523
47	347.388	316.896	346.280	316.967
48	346.889	316.999	346.242	316.383
49	346.948	317.176	345.895	316.692
50	346.991	316.592	346.160	316.741
51	346.181	316.075	345.865	316.190
52	345.959	316.641	346.125	316.589
53	346.434	316.749	346.198	316.687
54	346.059	316.670	346.500	316.915
55	346.354	316.873	346.756	317.099
56	347.259	317.051	346.595	316.856
57	347.069	317.201	346.585	316.694
58	346.743	317.464	346.657	316.620
59	346.398	316.766	346.416	316.444
60	346.553	316.947	345.414	316.303

---

UNCLASSIFIED

## Appendix C. Tabulated Data with Elevated Ground Plane Installed

Table 9: Tabulated data from tests at  $U_{ts} = 5$  m/s with the elevated ground plane installed

Time (s)	Baseline $q_{ts}$	Baseline $\Delta P$	Repeat $q_{ts}$	Repeat $\Delta P$
0	16.913	13.499	15.535	12.057
1	16.871	13.379	15.799	12.039
2	16.778	12.314	15.896	12.062
3	15.878	12.638	15.868	12.051
4	15.949	13.226	15.738	12.064
5	16.386	13.385	15.569	12.108
6	16.496	12.946	15.506	11.959
7	16.126	12.822	15.185	11.866
8	15.938	12.212	15.110	11.986
9	15.513	11.787	15.057	11.996
10	15.036	11.690	15.297	11.980
11	14.864	11.731	15.318	11.995
12	15.050	11.697	15.173	12.059
13	15.090	11.785	15.249	12.047
14	15.317	11.743	15.557	12.013
15	15.250	11.793	15.735	11.986
16	15.278	11.888	15.544	12.170
17	15.073	11.841	15.747	12.109
18	15.192	11.847	15.702	12.049
19	15.066	11.864	15.472	12.006
20	15.039	11.948	15.256	12.053
21	15.133	11.982	15.100	12.072
22	15.143	11.904	15.300	12.172
23	14.988	11.802	15.385	12.191
24	14.820	11.769	15.329	12.135
25	14.762	11.857	15.422	12.121
26	14.885	11.983	15.533	12.127
27	14.803	12.405	15.398	12.181
28	15.190	13.223	15.452	12.145
29	16.063	13.631	15.449	12.168
30	16.740	13.751	15.629	12.090
31	17.213	13.726	15.524	12.081
32	17.101	13.679	15.615	11.957
33	17.257	13.810	15.438	11.908
34	17.283	13.730	15.072	11.943
35	17.204	13.796	15.167	12.041
36	17.197	13.785	15.397	12.168
37	17.199	13.719	15.448	12.233

*Table 9 Continued: Tabulated data from tests at 5 m/s with the elevated ground plane installed*

38	17.194	13.645	15.489	12.121
39	17.126	13.475	15.616	11.989
40	16.946	12.617	15.490	12.007
41	16.178	12.190	15.639	12.130
42	15.623	12.138	15.510	12.113
43	15.364	12.106	15.511	12.071
44	15.310	12.161	15.698	12.129
45	15.339	12.231	15.599	12.097
46	15.681	12.299	15.858	11.966
47	15.783	12.286	15.542	11.865
48	15.520	12.372	15.321	11.785
49	15.326	12.361	15.243	11.840
50	15.541	12.412	15.413	11.850
51	15.573	12.319	15.147	11.836
52	15.494	12.274	14.947	11.966
53	15.220	12.810	15.275	12.010
54	15.618	13.277	15.418	11.977
55	16.316	13.251	15.458	11.981
56	16.479	13.099	15.356	11.977
57	16.281	12.627	15.324	11.972
58	15.849	12.420	15.376	11.970
59	15.672	12.520	15.167	11.844
60	15.617	12.681	15.206	11.810

Table 10: Tabulated data from tests at  $U_{ts} = 10$  m/s with the elevated ground plane installed

Time (s)	Baseline $q_{ts}$	Baseline $\Delta P$	Repeat $q_{ts}$	Repeat $\Delta P$
0	59.736	51.259	60.126	51.685
1	59.851	51.219	60.076	51.298
2	59.649	51.474	59.940	51.562
3	59.791	51.129	59.943	51.649
4	59.580	51.243	60.223	52.141
5	59.629	50.979	60.659	52.269
6	59.510	50.909	60.604	52.279
7	59.492	51.196	60.795	51.965
8	59.452	51.215	60.206	51.651
9	59.459	51.148	59.959	51.593
10	59.681	51.136	60.007	52.085
11	59.504	51.118	60.282	52.013
12	59.454	51.013	60.499	51.624
13	59.312	51.050	60.294	51.337
14	59.389	50.797	60.227	51.552
15	59.486	51.174	60.392	51.721
16	59.617	51.116	60.606	51.872
17	59.652	51.138	60.635	52.003
18	59.522	50.985	60.718	52.170
19	59.511	50.789	60.767	52.103
20	59.404	50.872	60.752	52.157
21	59.415	50.861	60.476	52.020
22	59.258	50.651	60.151	51.816
23	59.334	50.786	59.943	51.997
24	59.227	50.808	60.138	51.746
25	59.271	50.831	60.181	51.654
26	59.147	50.789	60.412	51.808
27	59.222	50.822	60.624	52.192
28	59.203	50.910	60.468	52.207
29	59.114	50.693	60.484	52.066
30	59.302	50.695	60.830	51.929
31	58.955	50.713	60.689	51.883
32	59.076	50.550	60.790	51.992
33	58.865	50.844	60.553	52.072
34	58.953	50.975	60.411	51.999
35	58.970	50.860	59.954	51.372
36	59.047	50.739	59.938	51.529
37	58.930	50.799	60.337	51.431
38	59.096	50.606	60.032	51.407
39	58.870	50.781	59.825	51.357
40	58.963	50.645	59.999	51.520

UNCLASSIFIED

DST-Group-TN-1728

Table 10 Continued: Tabulated data from tests at 10 m/s with the elevated ground plane installed

---

41	59.023	50.648	59.862	51.341
42	59.054	50.695	59.692	51.305
43	59.068	50.720	59.799	51.330
44	59.073	50.730	59.866	51.316
45	58.764	50.395	60.039	51.314
46	58.725	50.558	59.844	51.362
47	58.841	50.840	59.744	51.733
48	59.098	50.777	59.745	51.777
49	59.364	50.570	59.900	51.625
50	58.996	50.707	60.039	51.591
51	59.154	50.688	59.471	51.390
52	58.969	50.698	59.753	51.744
53	59.270	50.550	60.416	51.941
54	58.912	50.316	60.610	51.681
55	59.009	50.688	60.027	51.798
56	59.216	50.787	60.314	51.835
57	59.040	50.807	60.208	51.907
58	59.226	50.825	60.495	52.011
59	59.347	50.374	60.704	51.926
60	58.884	49.981	60.422	51.892

---

UNCLASSIFIED

Table 11: Tabulated data from tests at  $U_{ts} = 15$  m/s with the elevated ground plane installed

Time (s)	Baseline $q_{ts}$	Baseline $\Delta P$	Repeat $q_{ts}$	Repeat $\Delta P$
0	131.577	113.421	134.506	115.341
1	131.475	113.436	134.308	115.598
2	131.463	112.965	134.297	115.578
3	131.223	112.702	134.566	115.742
4	131.124	112.617	134.724	115.849
5	131.082	112.140	134.536	115.632
6	131.092	112.848	134.261	115.492
7	131.154	113.380	134.185	115.821
8	131.599	113.199	134.247	115.681
9	131.887	113.423	134.083	115.646
10	132.111	113.599	133.859	115.602
11	131.863	113.813	133.965	115.671
12	132.344	114.301	133.700	115.070
13	132.743	114.280	133.425	115.659
14	132.381	113.554	133.626	115.060
15	132.053	113.135	133.765	115.134
16	131.891	113.441	133.309	115.198
17	132.030	114.354	133.586	115.517
18	132.774	113.524	134.111	115.443
19	132.255	113.339	134.414	115.366
20	131.929	112.839	134.335	115.640
21	131.428	112.906	134.516	115.306
22	130.966	112.859	134.001	115.632
23	130.744	112.237	134.165	115.449
24	130.918	113.675	134.215	115.612
25	131.843	113.488	134.295	115.576
26	131.801	113.738	134.387	115.538
27	131.868	113.645	134.283	115.215
28	131.752	113.232	133.773	114.990
29	131.552	113.364	133.346	115.055
30	131.658	113.718	133.787	115.339
31	132.373	113.702	133.873	115.546
32	132.182	113.352	134.134	115.595
33	132.066	112.992	134.095	115.423
34	131.374	112.294	134.334	115.713
35	131.022	112.168	134.312	115.734
36	130.831	112.509	134.648	115.188
37	130.627	111.940	134.409	115.450
38	130.616	112.637	134.310	115.676
39	130.871	113.197	134.215	115.290
40	131.344	113.137	134.293	115.820

*Table 11 Continued: Tabulated data from tests at 15 m/s with the elevated ground plane installed*

41	131.708	113.681	134.138	115.542
42	131.833	113.553	134.156	115.611
43	131.956	113.439	134.119	115.810
44	131.983	113.161	134.333	115.362
45	131.825	112.936	134.092	115.531
46	131.542	112.701	133.897	115.294
47	131.192	113.143	133.511	115.320
48	131.393	113.227	133.731	115.672
49	131.644	113.138	133.894	115.287
50	131.541	112.137	134.015	115.550
51	130.737	110.984	134.178	115.396
52	129.583	111.772	134.444	116.038
53	130.066	112.276	134.538	115.611
54	130.364	112.300	134.635	115.375
55	130.602	112.613	134.304	115.611
56	131.096	113.159	133.986	115.548
57	131.708	113.492	134.165	115.413
58	131.911	113.058	133.880	115.553
59	131.610	112.926	133.776	115.242
60	131.675	113.249	133.787	115.494

Table 12: Tabulated data from tests at  $U_{ts} = 20$  m/s with the elevated ground plane installed

Time (s)	Baseline $q_{ts}$	Baseline $\Delta P$	Repeat $q_{ts}$	Repeat $\Delta P$
0	231.624	197.270	237.281	202.386
1	231.371	197.330	237.258	202.272
2	231.260	197.497	237.611	202.820
3	231.308	197.317	237.293	202.745
4	231.101	197.397	237.094	202.268
5	231.288	197.745	237.000	202.206
6	231.107	197.093	237.007	202.452
7	231.531	198.073	237.058	202.089
8	231.774	197.640	236.569	201.828
9	231.520	197.335	236.485	202.312
10	231.362	197.338	237.000	201.464
11	231.103	197.040	236.609	201.482
12	231.253	197.199	237.080	201.765
13	231.394	197.845	237.282	202.076
14	231.770	197.734	237.529	201.800
15	231.405	197.508	237.200	201.474
16	231.489	197.396	237.063	201.881
17	231.675	196.763	236.925	201.788
18	230.988	197.291	236.588	201.365
19	231.337	197.669	236.594	201.798
20	231.770	197.904	236.762	201.839
21	231.762	197.286	236.821	202.218
22	230.964	197.335	236.948	202.065
23	231.333	197.924	236.774	201.622
24	231.708	197.733	236.590	201.840
25	231.534	197.458	236.549	201.816
26	231.582	197.697	236.027	202.023
27	231.641	197.909	236.464	201.246
28	231.946	197.951	235.867	201.112
29	231.289	197.047	236.261	201.831
30	230.020	196.147	236.321	201.967
31	230.047	197.182	236.338	202.208
32	230.770	197.452	236.635	201.817
33	231.007	197.360	236.501	201.746
34	231.382	197.087	236.379	202.118
35	231.047	196.909	236.248	201.946
36	230.885	197.493	236.216	201.999
37	231.324	196.955	236.360	201.452
38	231.008	196.536	236.276	202.068
39	230.550	197.712	236.747	201.962
40	231.284	197.800	236.923	202.059

UNCLASSIFIED

DST-Group-TN-1728

Table 12 Continued: Tabulated data from tests at 20 m/s with the elevated ground plane installed

---

41	232.196	197.470	236.877	201.795
42	232.171	197.365	236.409	201.875
43	231.686	197.019	236.440	201.810
44	230.947	196.672	236.481	202.047
45	230.435	196.436	237.064	201.899
46	230.333	197.124	236.781	201.933
47	230.667	196.914	237.009	201.799
48	230.600	196.420	236.318	201.659
49	230.181	196.888	236.367	202.067
50	230.656	196.473	236.611	201.745
51	230.222	196.655	236.573	201.582
52	230.023	195.727	236.584	201.598
53	230.044	195.912	236.750	201.805
54	229.691	196.050	236.504	201.456
55	230.507	197.138	236.399	201.636
56	230.552	196.707	236.096	201.387
57	230.853	196.938	235.934	201.825
58	230.785	196.615	236.763	202.371
59	231.000	197.054	237.143	201.527
60	231.231	197.308	236.181	201.540

---

UNCLASSIFIED

Table 13: Tabulated data from tests at  $U_{ts} = 25$  m/s with the elevated ground plane installed

Time (s)	Baseline $q_{ts}$	Baseline $\Delta P$	Repeat $q_{ts}$	Repeat $\Delta P$
0	362.781	311.543	363.477	311.663
1	362.889	311.198	363.974	311.382
2	362.610	311.314	363.395	311.257
3	362.754	311.143	362.711	311.639
4	362.519	311.415	362.723	311.588
5	362.680	311.315	363.001	311.363
6	362.398	311.385	363.243	311.009
7	362.415	311.669	362.160	310.881
8	362.440	311.662	362.497	311.479
9	363.007	311.284	362.514	310.574
10	361.837	311.773	362.269	310.963
11	362.793	311.976	362.144	311.304
12	362.878	311.851	362.449	311.491
13	362.665	311.045	363.240	311.663
14	362.469	311.364	363.635	311.754
15	362.321	310.992	363.392	311.495
16	362.159	310.945	363.363	310.921
17	362.279	311.449	362.459	310.538
18	362.419	311.123	361.558	310.902
19	361.906	311.112	361.890	311.152
20	362.449	311.632	362.755	311.261
21	362.646	311.230	362.920	310.925
22	362.810	311.076	362.182	311.380
23	362.099	310.391	362.862	311.065
24	361.599	310.784	362.502	310.925
25	361.790	311.376	362.312	311.259
26	361.989	311.652	362.287	311.095
27	362.490	311.086	362.682	310.227
28	362.044	310.981	362.452	311.263
29	361.890	310.863	362.492	311.028
30	362.090	311.075	361.798	311.043
31	361.774	310.844	362.237	311.365
32	362.161	311.030	362.794	310.830
33	362.362	310.689	362.703	310.612
34	362.850	311.371	362.028	310.553
35	362.639	310.744	362.173	310.989
36	362.734	311.059	362.063	310.697
37	363.220	311.101	362.467	311.030
38	363.569	311.079	362.732	310.922
39	363.477	311.299	361.949	310.340
40	363.540	311.459	361.904	310.603

*Table 13 Continued: Tabulated data from tests at 25 m/s with the elevated ground plane installed*

41	363.452	311.441	361.854	310.636
42	362.936	311.259	362.264	310.760
43	362.188	309.431	362.864	310.958
44	361.327	310.821	362.889	310.897
45	361.973	311.777	362.400	310.702
46	362.413	311.267	362.297	310.784
47	362.397	310.899	361.925	310.791
48	362.371	311.078	361.858	310.666
49	362.434	311.174	362.456	310.951
50	362.092	311.454	362.263	310.871
51	362.110	311.017	362.477	310.791
52	361.967	311.269	362.585	310.660
53	362.720	310.983	362.178	310.851
54	362.378	311.518	362.514	311.119
55	363.211	311.240	362.447	310.802
56	363.527	311.376	362.421	310.440
57	363.307	311.176	361.859	311.059
58	362.896	311.108	362.206	310.601
59	362.490	310.673	361.806	310.510
60	362.102	310.636	361.607	310.290

**UNCLASSIFIED**

<b>DEFENCE SCIENCE AND TECHNOLOGY GROUP DOCUMENT CONTROL DATA</b>		1. DLM/CAVEAT (OF DOCUMENT)	
2. TITLE Calibration of the DST Group Research Wind Tunnel Pressure Rings		3. SECURITY CLASSIFICATION (FOR UNCLASSIFIED LIMITED RELEASE USE (L) NEXT TO DOCUMENT CLASSIFICATION)  Document (U) Title (U) Abstract (U)	
4. AUTHORS Jesse McCarthy		5. CORPORATE AUTHOR Defence Science and Technology Group 506 Lorimer St, Fishermans Bend, Victoria 3207, Australia	
6a. DST GROUP NUMBER DST-Group-TN-1728	6b. AR NUMBER 017-078	6c. TYPE OF REPORT Technical Note	7. DOCUMENT DATE February, 2018
8. OBJECTIVE ID		9. TASK NUMBER	10. TASK SPONSOR
11. MSTC Aircraft Performance and Survivability		12. STC Aerodynamics and Aeroelasticity	
13. DOWNGRADING/DELIMITING INSTRUCTIONS		14. RELEASE AUTHORITY Chief, Aerospace Division	
15. SECONDARY RELEASE STATEMENT OF THIS DOCUMENT  <i>Approved for Public Release</i>			
<small>OVERSEAS ENQUIRIES OUTSIDE STATED LIMITATIONS SHOULD BE REFERRED THROUGH DOCUMENT EXCHANGE, PO BOX 1500, EDINBURGH, SA 5111</small>			
16. DELIBERATE ANNOUNCEMENT No Limitations			
17. CITATION IN OTHER DOCUMENTS No Limitations			
18. RESEARCH LIBRARY THESAURUS Aerodynamics, Wind tunnels, Calibration, Flow measurement			
19. ABSTRACT A calibration of the pressure rings in the DST Group Research Wind Tunnel was performed for an empty test section and with an elevated ground plane installed. This pressure ring system is similar in principle to the piezo-rings utilised in the DST Group Low Speed Wind Tunnel for calculating nominal test-section wind speed with a calibration factor. Calibration factors were obtained for both the empty test section and when the elevated ground plane is installed. It is found that the addition of the elevated ground plane changes the calibration factor significantly.			

**UNCLASSIFIED**